Driving protein conformational changes with light: Photoinduced structural rearrangement in a heterobimetallic oxidase

Pearson T. Maugeri[a], Julia J. Griese[d,†], Rui M. Branca[e], Effie K. Miller[b], Zachary R. Smith[c], Jürgen Eirich[e], Martin Högbom*[d], Hannah S. Shafaat*[a,b,c]

[a]*Biophysics Graduate Program, The Ohio State University, Columbus, OH 43210, USA*

[b]*Ohio State Biochemistry Program, The Ohio State University, Columbus, OH 43210, USA*

[c]*Department of Chemistry and Biochemistry, The Ohio State University, Columbus, OH 43210, USA*

[d]*Department of Biochemistry and Biophysics, Stockholm University, SE-106 91 Stockholm, Sweden*

[e]*Department of Oncology–Pathology, Science for Life Laboratory, Karolinska Institutet, SE-17165 Stockholm, Sweden*

Supporting Information

Table of Contents

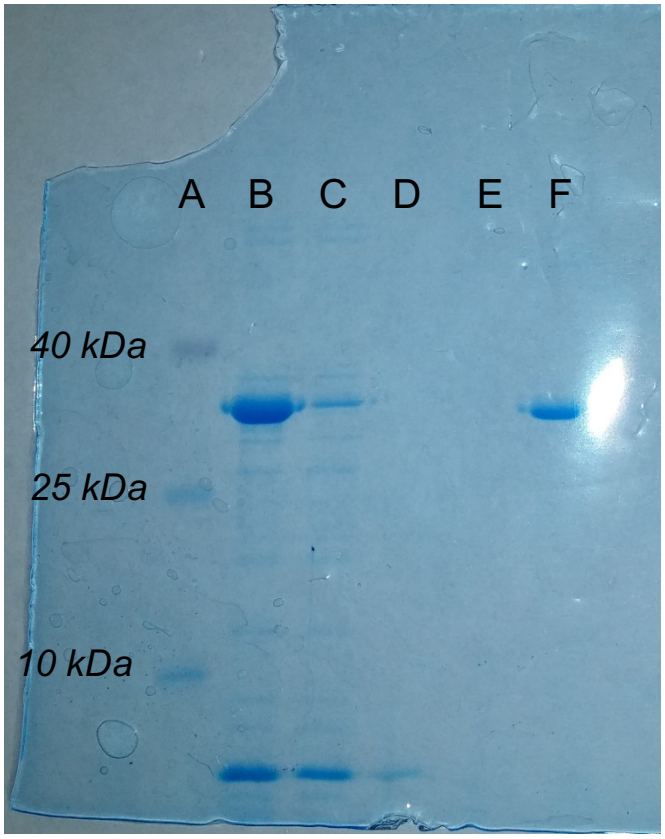

Lane	Sample
A	Protein Ladder (Spectra Multicolor Low Range, ThermoFisher Scientific)
B	Cell lysate
C	Column load flow through
D	Wash 1 with 25 mM HEPES, 40 mM imidazole, 300 mM NaCl, and 0.5 mM EDTA at pH 7.0
E	Wash 2 with 25 mM HEPES, 40 mM imidazole, and 300 mM NaCl at pH 7.0
F	Elution with 25 mM HEPES, 250 mM imidazole, and 300 mM NaCl at pH 7.0

Figure S1. Representative SDS-PAGE indicating R2lox expression and purification. Lanes are labeled as given in table.

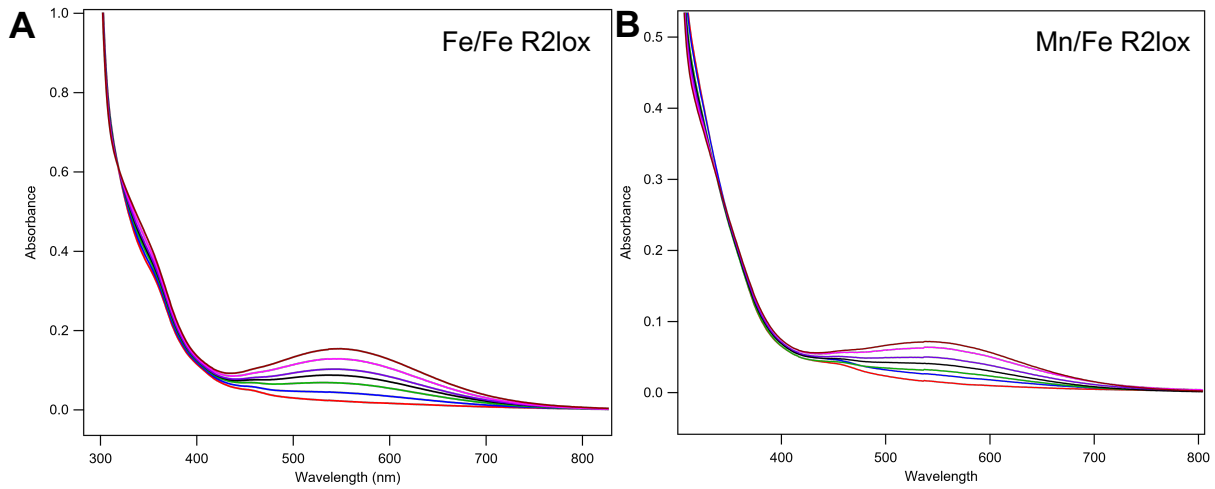

Figure S2. Representative spectra of photoconversion efficiency measurements for (A) Fe/Fe and (B) Mn/Fe R2lox showing spectral changes as a function of photolysis time from 0 min (red trace) – 30 min (brown trace).

Sample equations explaining how the quantum yield was calculated in this work.[1,2]

$$I = \frac{A_{510} v_2 v_3}{\varepsilon_{510} \Phi_{402} v_1 dt}$$

I = photon flux (einsteins/sec)
A = absorbance of $Fe^{II}(phen)_3^{2+}$ at 510 nm
v_2 = volume of ferrioxalate solution irradiated (L)
v_3 = volume of total solution after adding ferrioxalate (mL)
ε = molar extinction coefficient of $Fe^{II}(phen)_3^{2+}$ at 510 nm (1.1×10^4 $M^{-1}cm^{-1}$)
Φ = quantum yield of ferrioxalate Fe^{III} to Fe^{II} conversion (1.07 at 402 nm)
v_1 = volume of 1,10-phenanthroline solution added (mL)
d = path length of cuvette (1 cm)
t = time that ferrioxalate is irradiated (sec)

$$\Phi_{protein} = \frac{1}{f_m I} \frac{d[photoproduct]}{dt}$$

$$f_m = \frac{(1 - 10^{-A_{402,i}}) + (1 - 10^{-A_{402,f}})}{2}$$

f_m = fraction of molecules that absorb light
$A_{402,i}$ = absorbance at 402 nm of intial spectrum
$A_{402,f}$ = absorbance at 402 nm of final spectrum

Table S1. Crystallographic statistics for dark and photoconverted Fe/Fe R2lox.

State	**dark state**	**photoconverted**
Beamline	X06DA/SLS	X06DA/SLS
Wavelength (Å)	1.00	1.00
Resolution range (Å)	50.00-1.70 (1.81-1.70)	50.00-2.00 (2.13-2.00)
Space group	I222	I222
Unit cell dimensions a, b, c (Å)	55.67,96.62, 128.40	55.63, 97.31, 127.98
Unique reflections	38162 (6063)	23693 (3747)
Multiplicity	6.6	6.6
Completeness (%)	99.8 (99.0)	99.8 (98.9)
$I/\sigma(I)$	12.00 (0.55)	11.37 (0.77)
R_{merge} (%)	11.3 (307.7)	13.7 (232.5)
R_{meas} (%)	12.3 (335.3)	14.9 (252.0)
$CC_{1/2}$ [§]	99.9 (12.1)	99.9 (32.3)

Values in parentheses are for the highest resolution shell. Friedel pairs were merged. [§]Percentage of correlation between intensities from random half-datasets.[3] The correlation is significant at the 0.1% level in all resolution shells in all datasets.

Table S2. Refinement statistics for crystal structures of dark and photoconverted Fe/Fe R2lox.

State	**dark state**	**photoconverted**
PDB ID	5OMK	5OMJ
Resolution range (Å)	48.31-1.70	48.66-2.01
Reflections used	38157	23651
R_{work}/R_{free} (%)†	17.8/20.9	20.2/26.4
Coordinate error (Å)	0.28	0.43
Non-H atoms	2486	2430
Protein residues‡	285 (2-286)	285 (2-286)
Water molecules	101	52
Ligand molecules	1	1
Metal ions	2	2
rmsd bonds (Å)¶	0.013	0.017
rmsd angles (°)¶	1.075	1.187
Ramachandran favored/allowed/ outliers (%)‖	98.2/1.4/0.4	94.6/5.4/0.0
Clashscore‖	2.07	5.94
Wilson *B* factor (Å^2)	34.1	43.9
Average *B* factors (Å^2)&		
all atoms	46.4	61.5
protein main and side chains	46.4	61.7
site 1 Fe ion	30.0	40.0
site 2 Fe ion	30.6	43.0
ligand	49.3	59.7
water	44.8	45.3

†Rfree is calculated from a randomly selected subset of ~2000 reflections (corresponding to ≤5% of reflections) excluded from refinement. ‡Residues out of the 302 residue full-length protein included in the final model are given in parentheses. ¶Root-mean-square deviation from ideal geometry. ‖Geometry statistics were calculated with MolProbity.[4] &Average *B* factors were calculated with $B_{average}$ in the CCP4 suite.[5]

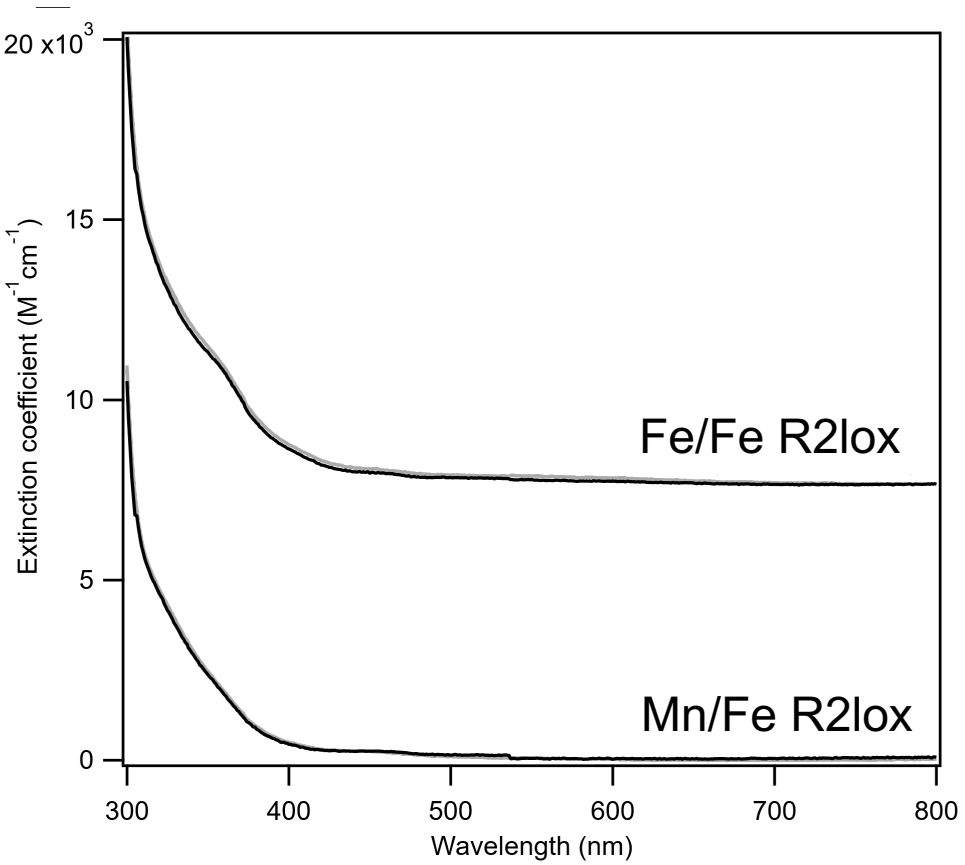

Figure S3. Photoconversion control experiments showing (*top*) WT Fe/Fe and(*bottom*) Mn/Fe R2lox immediately following reconstitution (black) and after 30 days in the dark (grey).

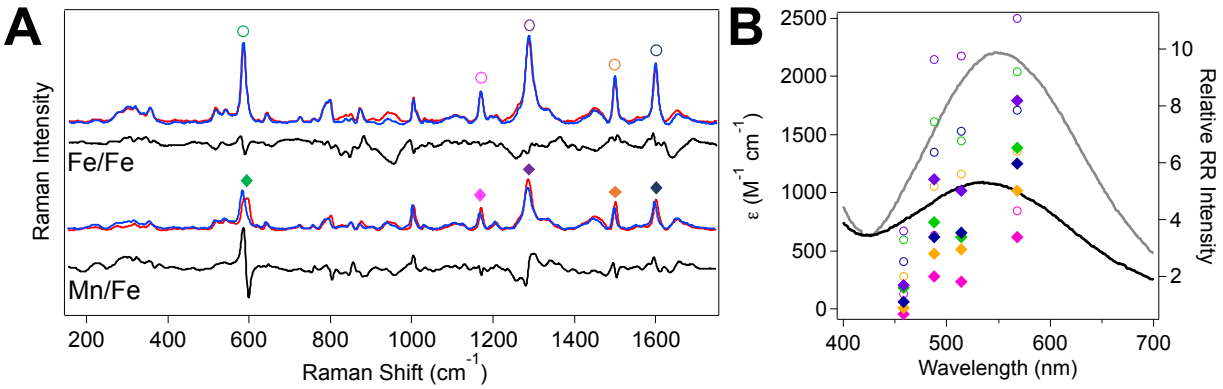

Figure S4. (**A**) Resonance Raman spectra of photoconverted Fe/Fe (top) and Mn/Fe (bottom) R2lox (λ_{ex} = 457.9 nm, P_{ex} = 25 mW, T = 298 K) prepared in H_2O (blue) and D_2O (red) buffers. Black traces show the isotopic difference spectra (H_2O-D_2O). (**B**) Resonance Raman excitation profiles for key vibrational modes overlaid with the absorption spectra of photoconverted Fe/Fe (grey) and Mn/Fe (black) R2lox. The bands represented in the resonance Raman excitation profiles are tagged in the RR spectra with the respective symbols.

Table S3. Extinction coefficients of various purple acid phosphatases.

Species of origin	**Metal centers**	**λ_{max} (nm)**	**Extinction coefficient (M^{-1} cm^{-1})**
Sus scrofa (pig)	Fe^{III}/Fe^{III}	545 [6]	3100 [6]
Phaseolus vulgaris (red kidney bean)	Fe^{III}/Zn^{II}	560 [7]	3360 [7]
Ipomoea batatas (sweet potato)	Fe^{III}/Mn^{II}	560 [8]	3207 [8]

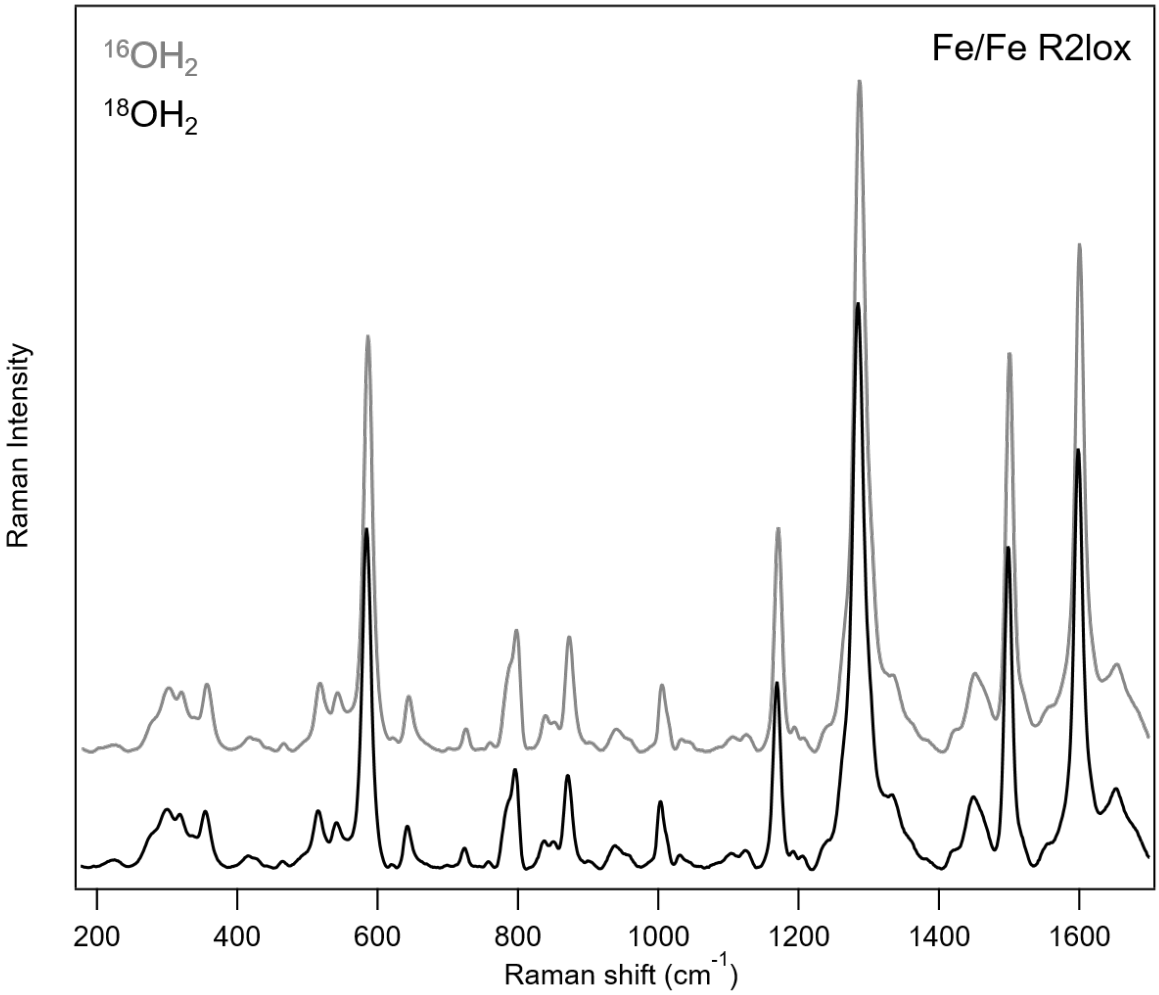

Figure S5. Resonance Raman spectra of photoconverted WT Fe/Fe R2lox prepared in natural abundance $H_2{}^{16}O$ buffer (grey) and exchanged into $H_2{}^{18}O$ buffer (black) prior to photolysis (RR λ_{ex} = 457.9 nm, P = 25 mW, T = 298 K).

Table S4. Quantum yields for photoconversion of R2lox mutants.

	WT	***V72A***	***V72L***	***V72I***	***Y175F***	***Y162F***
Mn/Fe	3.1% ± 0.26%	3.4% ± 1.3%	3.6% ± 0.18%	7.2% ± 0.94%	1.5% ± 0.22%	0%
Fe/Fe	2.3% ± 0.09%	2.9% ± 0.38%	2.7% ± 0.21%	3.1% ± 0.27%	2.0% ± 0.22%	0%

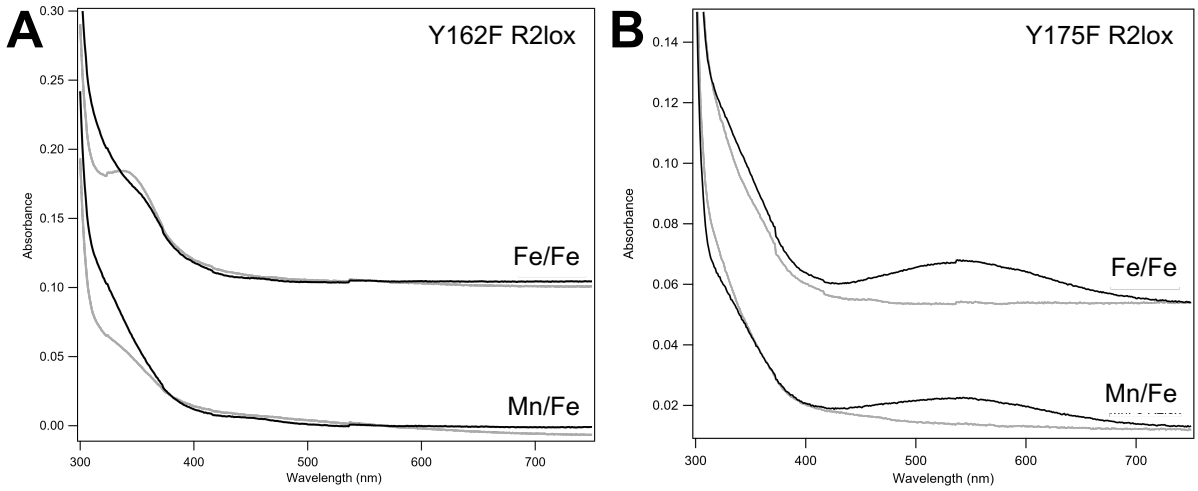

Figure S6. Absorption spectra of 20 μM (A) Y162F and (B) Y175F R2lox variants prior to photolysis (grey) and after irradiation (black).

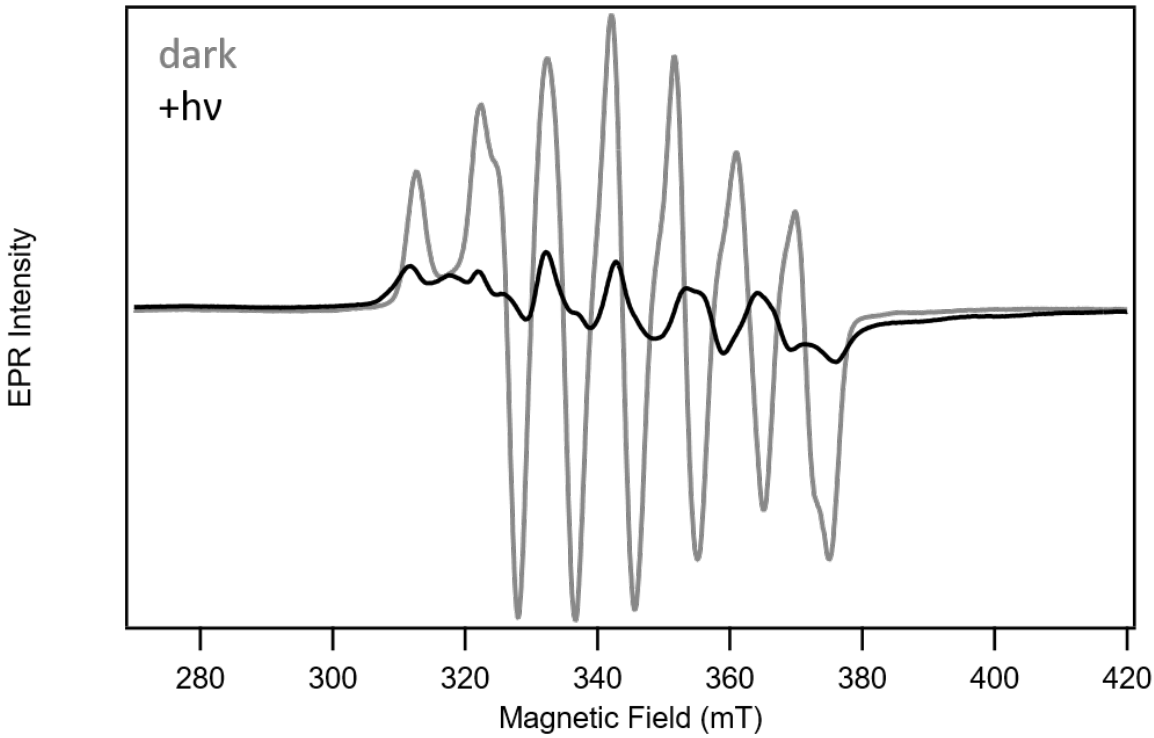

Figure S7. CW X–band EPR spectra (T = 5 K) of Y162F Mn/Fe R2lox prior to (grey) and following (black) irradiation.

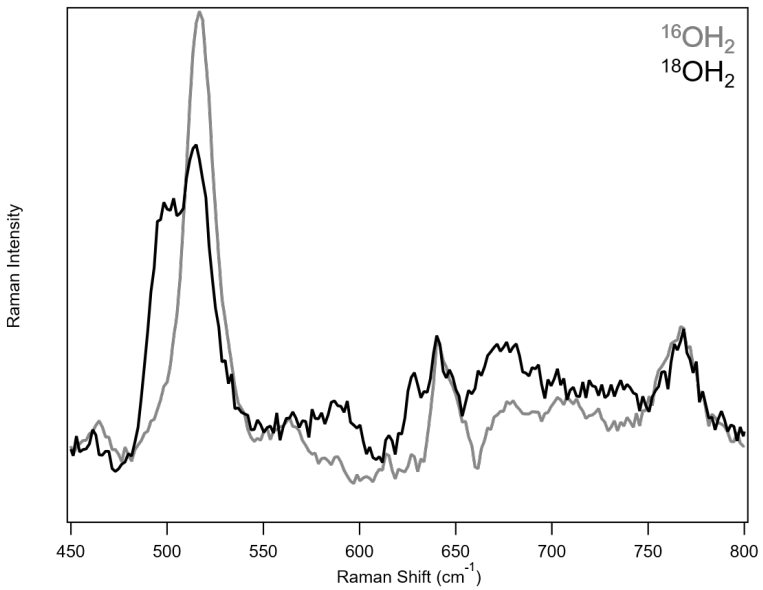

Figure S8. The resonance Raman spectrum of Y162F Fe/Fe R2lox in buffer prepared with natural abundance ($H_2{}^{16}O$, grey) and $H_2{}^{18}O$-enriched (black) water (λ_{ex} = 407 nm, P = 10 mW, T = 298 K).

Annotated MS2 spectrum of the AVIRAATVYNMIVE(-CO2)GTLAE peptide

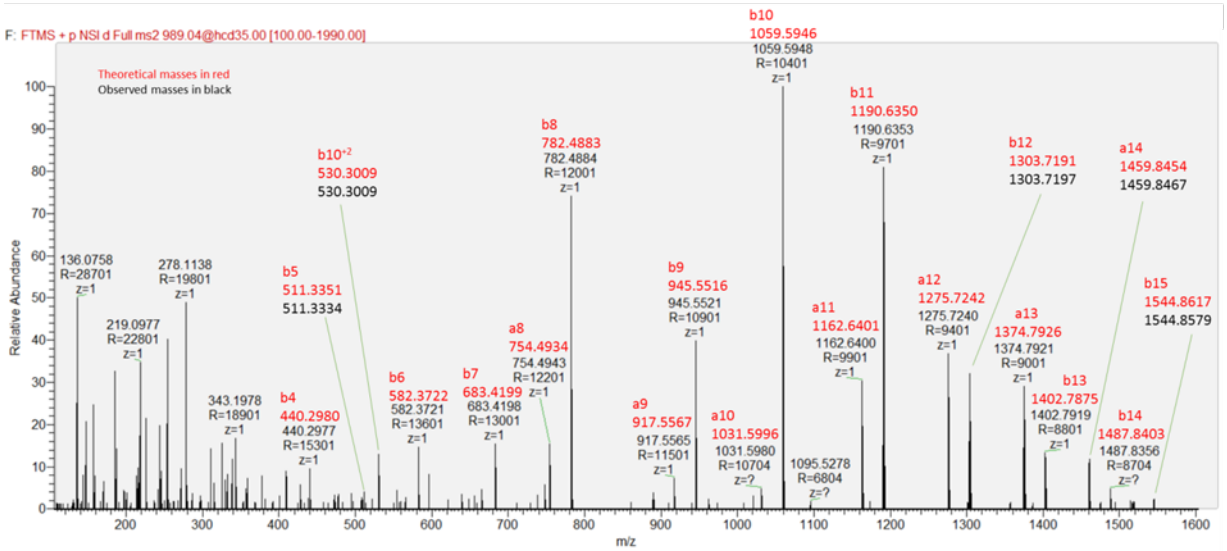

a	b	N-terminal	-	C-terminal	y
---	---	1	A	19	---
143.1179	171.1128	2	V	18	1906.0466
256.2020	284.1969	3	I	17	1806.9782
412.3031	440.2980	4	R	16	1693.8942
483.3402	511.3351	5	A	15	1537.7931
554.3773	582.3722	6	A	14	1466.7559
655.4250	683.4199	7	T	13	1395.7188
754.4934	782.4883	8	V	12	1294.6712
917.5567	945.5516	9	Y	11	1195.6027
1031.5996	1059.5946	10	N	10	1032.5394
1162.6401	1190.6350	11	M	9	918.4965
1275.7242	1303.7191	12	I	8	787.4560
1374.7926	1402.7875	13	V	7	674.3719
1459.8454	1487.8403	14	E(-43.989829)	6	575.3035
1516.8668	1544.8617	15	G	5	490.2508
1617.9145	1645.9094	16	T	4	433.2293
1730.9986	1758.9935	17	L	3	332.1816
1802.0357	1830.0306	18	A	2	219.0975
---	---	19	E	1	148.0604

Figure S9. Annotated MS2 fragmentation spectrum of the doubly charged precursor ion 989.0422 m/z and respective theoretical fragment ion table of the peptide AVIRAATVYNMIVE(-CO_2)GTLAE with the decarboxylated glutamate residue. The peptide was obtained by proteolytic digestion with Glu-C of irradiated R2lox protein. The experimental m/z values are in black, whereas the annotation and theoretical m/z values are shown in red. The mass error is typically less than 0.01 m/z, in accordance with the high resolution used (17,500). Among the fragment ions observed, the most important are a14, b14 and b15 which demonstrate the decarboxylated glutamate residue (E167).

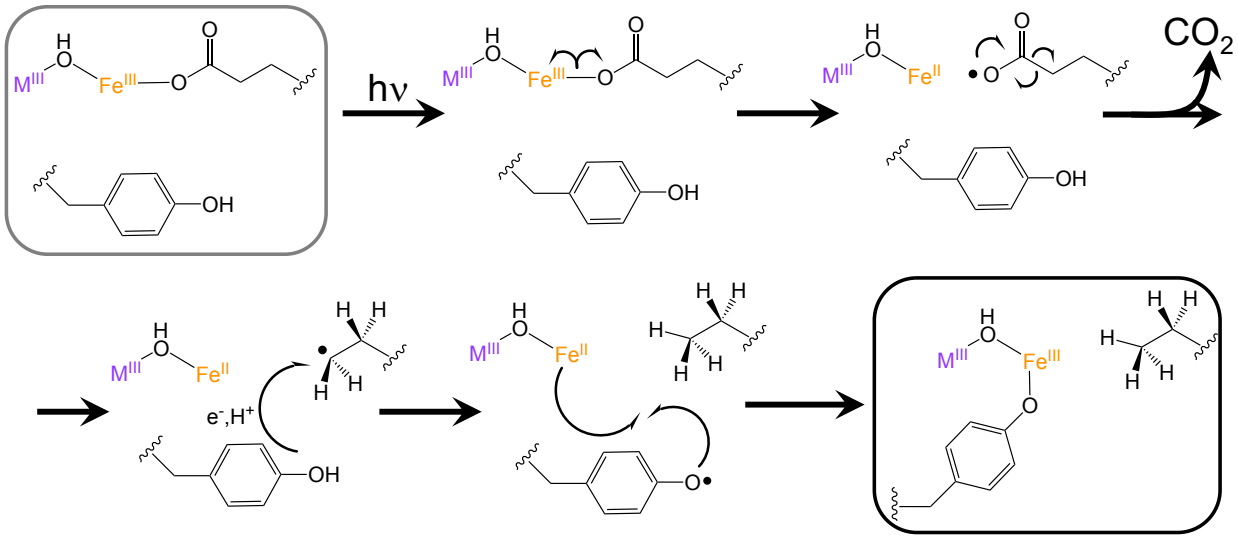

Figure S10. Scheme for photoconversion of R2lox variants lacking Y162-V72 crosslink.

Supplemental References

(1) Murov, S. L.; Carmichael, I.; Hug, G. L. *Handbook of Photochemistry, 2nd edition*, 2nd ed.; Marcel Dekker, Inc.: New York, NY, 1993.
(2) Ma, X.; Tian, H. *Photochemistry and Photophysics. Concepts, Research, Applications. By Vincenzo Balzani, Paola Ceroni and Alberto Juris.*; Wiley-VCH Verlag: Weinheim, Germany, 2014.
(3) Karplus, P. A.; Diederichs, K. *Science* **2012**, *336*, 1030–1033.
(4) Chen, V. B.; Arendall, W. B.; Headd, J. J.; Keedy, D. A.; Immormino, R. M.; Kapral, G. J.; Murray, L. W.; Richardson, J. S.; Richardson, D. C. *Acta Crystallogr. D Biol. Crystallogr.* **2010**, *66*, 12–21.
(5) Winn, M. D.; Ballard, C. C.; Cowtan, K. D.; Dodson, E. J.; Emsley, P.; Evans, P. R.; Keegan, R. M.; Krissinel, E. B.; Leslie, A. G. W.; McCoy, A.; McNicholas, S. J.; Murshudov, G. N.; Pannu, N. S.; Potterton, E. A.; Powell, H. R.; Read, R. J.; Vagin, A.; Wilson, K. S. *Acta Crystallogr. D Biol. Crystallogr.* **2011**, *67*, 235–242.
(6) Antanaitis, B. C.; Strekas, T.; Aisen, P. *J. Biol. Chem.* **1982**, *257*, 3766–3770.
(7) Beck, J. L.; McConachie, L. A.; Summors, A. C.; Arnold, W. N.; De Jersey, J.; Zerner, B. *Biochim. Biophys. Acta BBA - Protein Struct. Mol. Enzymol.* **1986**, *869*, 61–68.
(8) Schenk, G.; Boutchard, C. L.; Carrington, L. E.; Noble, C. J.; Moubaraki, B.; Murray, K. S.; De Jersey, J.; Hanson, G. R.; Hamilton, S. *J. Biol. Chem.* **2001**, *276*, 19084–19088.